

## Low-Speed Flotation Equilibrium of Macromolecules in the Analytical Ultracentrifuge

Stephen E. Harding,\* Peter J. Morgan,

*Department of Applied Biochemistry and Food Science, University of Nottingham,  
Sutton Bonington LE12 5RD, U.K.*

and Karel Petrak

*Advanced Drug Delivery Research Unit, Ciba-Geigy Pharmaceuticals Ltd., Wimbleshurst Road,  
Horsham, W. Sussex, RH12 5AB, U.K. (Received: March 29, 1989)*

The application of low-speed flotation equilibrium in the analytical ultracentrifuge for molecular weight analysis of a system of macromolecules in solvent of higher density is described. The method is illustrated by application to a poly[(isoprene)-*b*-(ethylene oxide)] block copolymer system in chloroform. Solute distributions recorded by using Rayleigh interference optics and the determination of weight-average molecular weights (both "whole-cell" and "point" averages) are specifically considered, although extension of the method to data recorded from other optical systems (namely, absorption and Schlieren) and for the determination of other averages (number, *z*, etc.) is indicated. The results are compared with a conventional low-speed sedimentation equilibrium of this polymer with water as solvent, where the polymer forms micelles. From comparison of the two results an estimate for the aggregation number is given for the micelles.

### Introduction

Sedimentation equilibrium techniques in the analytical ultracentrifuge have provided powerful methods for obtaining among other information molecular weight averages (see, e.g., ref 1), polydispersity,<sup>2</sup> and interaction phenomena<sup>3</sup> of macromolecular solutions.

The routine use of these procedures for molecular weight analysis has declined in recent times, particularly with the advent in the protein biochemistry field of the relative technique of sodium dodecyl sulfate-polyacrylamide gel electrophoresis. In characterizing synthetic polymers, it has also increasingly become a "Cinderella" technique, largely because of the advent of light scattering methods and gel permeation chromatography (GPC) with very few recent examples in the literature of its use. Despite this, sedimentation equilibrium remains for many polymer systems—particularly difficult heterogeneous systems—an intrinsically more suitable technique; for example, it does not suffer from problems of sample clarification which are crucial for light scattering<sup>4</sup> or problems of calibration and polymer/column interactions as in GPC.<sup>5</sup>

We now report, for the first time as far as we are aware, the application of *low-speed* (as opposed to "high-speed" or "meniscus depletion") sedimentation equilibrium procedures for the molecular weight analysis of polymers whose density is less than that of the solvent in which they are dispersed. Since the direction of "sedimentation" is for these systems in the opposite direction to the direction of the centrifugal field, we will henceforth refer to the method as "*low-speed flotation equilibrium*". Nelson et al.<sup>6</sup> have previously reported the application of high-speed or "meniscus depletion"<sup>7</sup> flotation equilibrium to the study of low-density lipoproteins (LDL's). The depletion method avoids the need to determine meniscus concentrations, but a number of stringent criteria have to be satisfied<sup>2,8</sup> and in many applications—particularly for highly polydisperse systems where it is often impossible to deplete properly the meniscus without losing optical registration of the Rayleigh interference fringes at the cell base (see, e.g., ref 9)—the method is not suitable.

For this reason, and since polydispersity is the hallmark of many classes of macromolecule (including lipoproteins), we have investigated the use of the more applicable low-speed flotation equilibrium for such solutions.

As with low-speed sedimentation equilibrium the meniscus concentration (for flotation, the concentration at the cell base) remains finite, but the same routine methods can be applied for its extraction [involving for example mathematical manipulation

of the basic fringe data<sup>10,11</sup> or use of a synthetic boundary cell (see, for example, ref 9 and 12)].

In all that follows we restrict our analysis to solute distributions at flotation equilibrium recorded using the Rayleigh interference optical system, although the treatment can be readily extended to data recorded using other optical systems. We also consider explicitly the evaluation of only one particular type of average molecular weight, the weight average [since this is the average directly determinable from the Rayleigh system without the problems of difficult integrations and extrapolations (number averages) or double differentiation of the basic fringe data (*z* averages)]. The results can be easily extended however to the latter case, particularly *z* averages (directly determinable by using the Schlieren optical system and the "Lamm" plot<sup>9</sup>).

### Theory

*Low-Speed Sedimentation Equilibrium.* We give a brief summary of some of the salient features of conventional low-speed sedimentation equilibrium (see, for example, Creeth and Pain's review<sup>9</sup> for a more complete description). Denoting absolute concentrations (in terms of fringes at various radial positions, *r*) as *J* and concentrations relative to that at the meniscus (*r* = *a*) as *j* [thus  $J(r) = J(a) + j(r)$ ], the fundamental differential equation of sedimentation equilibrium for an ideal system can be written<sup>9,13</sup>

$$\frac{J(r)}{A_n(r)} - \frac{J(a)}{A_n(a)} = 2 \int_a^r rJ \, dr = J(a)(r^2 - a^2) + 2 \int_a^r rj \, dr \quad (1)$$

where  $A_n$  is the reduced number-average molecular weight. For

- (1) Teller, D. C. *Methods Enzymol.* **1973**, 27, 346.
- (2) Fujita, H. *Foundations of Ultracentrifuge Analysis*; Wiley: New York, 1975; Chapter 5.
- (3) Kim, H.; Denonier, R. C.; Williams, J. W. *Chem. Rev.* **1977**, 77, 659.
- (4) Huglin, M. B. *Light Scattering from Polymer Solutions*; Academic Press: London, 1972.
- (5) Barth, J. G. *J. Chromatogr. Sci.* **1980**, 18, 409.
- (6) Nelson, C. A.; Lee, J. A.; Brewster, M.; Morris, M. D. *Anal. Biochem.* **1974**, 59, 69.
- (7) Strictly speaking, "base depletion" in this case.
- (8) Yphantis, D. A. *Biochemistry* **1964**, 3, 297.
- (9) Creeth, J. M.; Pain, R. H. *Prog. Biophys. Mol. Biol.* **1967**, 17, 217.
- (10) Teller, D. C.; Horbett, J. A.; Richards, E. G.; Schachman, H. K. *Ann. N.Y. Acad. Sci.* **1969**, 164, 66.
- (11) Creeth, J. M.; Harding, S. E. *J. Biochem. Biophys. Methods* **1982**, 7, 25.
- (12) Nureddin, A.; Johnson, P. *Biochemistry* **1977**, 16, 1730.
- (13) Creeth, J. M. *Biochem. Soc. Trans.* **1980**, 8, 520.

\* To whom correspondence should be addressed.

a nonideal system the  $A_n$  are apparent values.

Molecular weight averages are related to "reduced" molecular weight averages,  $A_i$ , by<sup>11,14</sup>

$$A_i = k_i M_i \quad (2)$$

where  $i$  represents a particular average (number,  $n$ ; weight,  $w$ ;  $z$ , etc.; the star operational point average,  $*$ ) and  $k_i$  is given by

$$k_i = \frac{(1 - \bar{v}_i \rho) \omega^2}{2RT} \quad (2')$$

where the symbols have their usual significance. The reduced star average,  $A^*$ , has several useful properties for the analysis of sedimentation equilibrium data<sup>11</sup> and is defined by

$$A^*(r) = \frac{A_n(r) A_n(a)}{A_n(a) J(r) - A_n(r) J(a)} j(r) \quad (3)$$

and hence eq 1 becomes

$$j(r)/A^*(r) = J(a)(r^2 - a^2) + 2 \int_a^r rj \, dr \quad (4)$$

A graph of  $j/(r^2 - a^2)$  vs  $\int_a^r rj \, dr/(r^2 - a^2)$  therefore has a limiting slope of  $2A^*(a)$  and intercept  $A^*(a) \cdot J(a)$  and hence the meniscus concentration  $J(a)$  can be found. Teller et al.<sup>10</sup> list other manipulations of the basic equation for sedimentation equilibrium which similarly yield  $J(a)$ .

Among the useful properties of the  $A^*$  function<sup>11</sup> is that it facilitates the determination of the (reduced) point weight-average molecular weight over the whole solute distribution,  $A_w^\circ$ :

$$\frac{j(b)}{A^*(b)} = J(a)(b^2 - a^2) + 2 \int_a^b rj \, dr \quad (5)$$

where  $j(b)$  is the concentration at the cell base relative to the concentration at the meniscus. The reduced weight-average molecular weight over the whole cell,  $A_w^\circ$ , is<sup>9</sup>

$$A_w^\circ = \frac{J(b) - J(a)}{J_0(b^2 - a^2)} = \frac{j(b)}{J_0(b^2 - a^2)} \quad (6)$$

where  $J_0$  is the initial loading concentration. By use of eq 4 and the usual conservation of mass equation  $[J_0(b^2 - a^2)]/2 = \int_a^b rJ \, dr$  it follows that<sup>11</sup>

$$A^*(b) = A_w^\circ \quad (7)$$

where  $b$  is the radial position at the cell base and  $J_0$  is the initial loading concentration in fringe numbers.  $A_w^\circ$ , and hence  $M_w^\circ$ , can therefore be obtained either by extrapolation of the  $A^*$  (or  $M^*$ ) function to the cell base (eq 7) or by direct use of eq 6. The latter requires the more difficult extrapolation of  $\ln J$  to the cell base: in general, the  $M^*$  method provides the more reliable extraction procedure for  $M_w^\circ$ , particularly for heterogeneous or strongly nonideal systems.<sup>11</sup>

Point weight-average (apparent) molecular weights can be obtained from the equation

$$A_w = d \ln J / dr^2 \quad (8)$$

(cf. ref 9, eq 2.10).

**Low-Speed Flotation Equilibrium.** For the case of low-speed flotation equilibrium the constant  $k_i$  in eq 2 becomes negative, since  $\bar{v}_i \rho > 1$  and the solute distribution is such that there is a higher concentration at the air/solution meniscus ( $r = a$ ) relative to the cell base ( $r = b$ ). The fundamental equation of sedimentation equilibrium (cf. eq 1) still applies for the redistribution of solute except that the redistribution is now relative to the cell base ( $r = b$ ) and solute concentrations are higher at the solution/air meniscus ( $r = a$ ). Equations 1 and 3-6 become for this case

$$\frac{J(r)}{A_n(r)} - \frac{J(b)}{A_n(b)} = 2 \int_b^r rJ \, dr = J(b)(r^2 - b^2) + 2 \int_b^r rj \, dr \quad (9)$$

$$A^*(r) = \frac{A_n(r) A_n(b)}{[A_n(b) J(r) - A_n(r) J(b)]} j(r) \quad (10)$$

$$\frac{j(r)}{A^*(r)} = J(b)(r^2 - b^2) + 2 \int_b^r rj \, dr \quad (11)$$

$$\frac{j(a)}{A^*(a)} = J(b)(a^2 - b^2) + 2 \int_b^a rj \, dr \quad (12)$$

$$A_w^\circ = \frac{J(a) - J(b)}{J_0(a^2 - b^2)} = \frac{j(a)}{J_0(a^2 - b^2)} \quad (13)$$

$$A^*(a) = A_w^\circ \quad (14)$$

Equation 8 applies also to the flotation case. All the reduced average molecular weights ( $A_i$ ), including  $A^*$ , will be negative.

**Thermodynamic Nonideality.** In all the above the same problems concerning activity coefficients and thermodynamic nonideality apply and have to be taken into account: failure to do so, as with conventional equilibrium, can lead to erroneous results. Such effects can be minimized however by using very low solute concentrations ( $\sim 0.2$  mg/mL) and long (e.g., 30 mm) path length cells. Further, in severe cases measurement at several concentrations and extrapolation to zero concentration are necessary. For this, the use of ultrashort columns (cf. van Holde and Baldwin methods I and III;<sup>15</sup> see also ref 9) and Yphantis style multichannel centerpieces<sup>1,8,16</sup> are of value. The use of short columns ( $\sim 2$  mm) and low speeds is particularly suited to polydisperse materials where nonideality effects can be enhanced<sup>2</sup> for high values of the parameter  $\lambda = (1 - \bar{v}_i \rho) \omega^2 (r_2^2 - r_1^2) / 2RT$  where  $\omega$  is the angular velocity,  $r_1$  the radial position at the meniscus (or base for flotation), and  $r_2$  the radial position at the base (meniscus).

## Experimental Section

**Materials.** Poly[(isoprene)-*b*-(ethylene oxide)] block copolymer (Copo 9) was obtained from Prof. Riess and Dr. Abou Madi (Ecole Nationale Supérieure de Chimie, Mulhouse, France) under a collaborative agreement. The chemical composition of the polymer was as follows (%): C, 65.8; H, 10.1; O, 23.4. By use of these values, the mean calculated content (% w/w) of isoprene in the copolymer was 34.5.

Two solvents were used: unbuffered deionized distilled water for conventional sedimentation equilibrium and chloroform (CHCl<sub>3</sub>, AnalaR grade) for flotation equilibrium. The polymer was dissolved in water by heating to 80 °C for 30 min and constant stirring overnight at ambient temperature leaving a nonturbid solution. The polymer readily dissolved in CHCl<sub>3</sub> at ambient temperature.

**Low-Speed Sedimentation/Flotation Equilibrium.** A Beckman Model E analytical ultracentrifuge was employed equipped with a He-Ne laser light source (5 mW, 632.18 nm) and an RTIC temperature measuring system. Cells of 30-mm optical path length were employed using either aluminum filled epoxy (for aqueous solvent) or Kel F (for chloroform) centerpieces. Determinations were made at 1961 rpm (Copo 9 in H<sub>2</sub>O) and 19 130 rpm (Copo 9 in CHCl<sub>3</sub>) at 20.0 °C. Solution columns of  $\sim 2$ -mm length were used. For Copo 9 in CHCl<sub>3</sub> a loading concentration of  $\sim 1.0$  mg/mL was employed; in water a similar concentration was used (which ensured the formation of micelles).  $M_w^\circ$  values were extracted from the  $A^*$  (or equivalently the  $M^*$ ) function as described above, and point weight-average molecular weights were obtained by using sliding strip quadratic fits to the observed fringe data (see, e.g., ref 1). The partial specific volume,  $\bar{v}$ , was determined from density increments by means of an Anton-Paar precision density meter<sup>17</sup> calibrated with CsCl standards.<sup>18</sup> For

(15) Van Holde, K. E.; Baldwin, R. L. *J. Phys. Chem.* **1958**, *62*, 734.

(16) Yphantis, D. A. *Ann. N.Y. Acad. Sci.* **1960**, *88*, 586.

(17) Kratky, O.; Leopold, A.; Stabinger, H. *Methods Enzymol.* **1973**, *270*,

48.

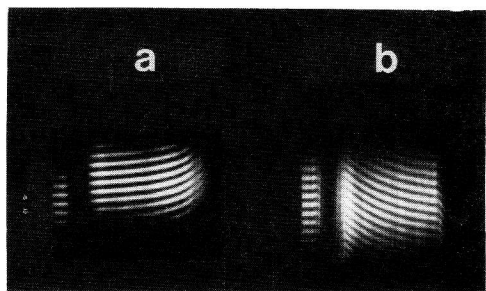


**Figure 1.** Rayleigh interference sedimentation equilibrium patterns: (a) Copo 9 in water. Initial loading concentration,  $c^{\circ}$ ,  $\sim 1.0$  mg/mL; rotor speed = 1961 rpm; temperature = 20.0 °C. (b) Copo 9 in chloroform.  $c^{\circ} \sim 1.0$  mg/mL; rotor speed = 19 139 rpm; temperature = 20.0 °C.

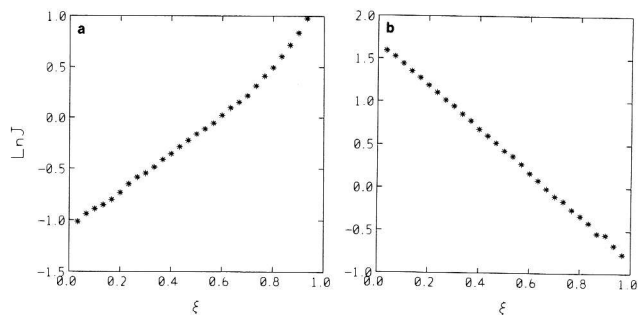


**Figure 2.** Plots of log fringe concentration vs the radial displacement-squared parameter  $\xi = (r^2 - a^2)/(b^2 - a^2)$ : (a) Copo 9 in water; (b) Copo 9 in chloroform. Other details as in Figure 1.

this study the  $\bar{v}$  was assumed constant for the polymer in the two solvents.

## Results

A direct comparison of the Rayleigh/interference patterns for the two cases of sedimentation and flotation equilibrium is given in Figure 1, a and b, respectively; opposite curvature for Figure 1b is apparent. It is also apparent that, in spite of the low speed (1961 rpm), near-meniscus depletion conditions were obtained for Copo 9 in water: a value for  $J_a$  of  $\sim 0.33$  was found by using the method of Creeth and Harding.<sup>11</sup>

By analogy, for the case of flotation equilibrium of the polymer in chloroform the absolute fringe concentration at the cell base,  $J_b$  of  $\sim 2.2$  (fringe no.), was obtained from the ratio of (twice) the intercept to the limiting slope of a plot of  $j/(r^2 - b^2)$  vs  $\int_b^r rj dr/(r^2 - b^2)$  (cf. ref 11).

Plots of  $\ln J$ , the logarithm of the (absolute) fringe concentration  $J$ , vs the radial displacement squared parameter,  $\xi$ , are given for Copo 9 in water (Figure 2a) and for the flotation equilibrium of Copo 9 in  $\text{CHCl}_3$  (Figure 2b). Besides the obvious negative slope for the polymer in chloroform, what is most notable about these two plots is that in chloroform the plot is approximately linear, whereas for the case of water upward curvature near the cell base is clearly evident, characteristic of heterogeneity (although this could be masked, in Figure 2b, by thermodynamic nonideality).

(Apparent) whole-cell weight-average molecular weight values  $M_w^{\circ}$  were obtained from extrapolation of  $M^*$  to the cell meniscus ( $r = a$ ;  $\xi = 0$ ) for flotation equilibrium (Figure 3b) and to the cell base ( $r = b$ ;  $\xi = 1$ ) for sedimentation equilibrium (Figure 3a). Values of  $M_w^{\circ}$  of  $35\,000 \pm 2\,000$  for Copo 9 in  $\text{CHCl}_3$  (corresponding to the unimer form) compared to  $(15.0 \pm 3.0) \times 10^6$  for Copo 9 in water were obtained. The greater uncertainty in the value in water is chiefly a consequence of the small value for the buoyancy factor ( $1 - \bar{v}\rho_0 = 0.0808$  at 20.0 °C) compared with the buoyancy factor in chloroform, whose value at 20.0 °C is  $-0.371$ , and also the more difficult extrapolation of  $M^*$  to cell base. The two values for the weight-average  $M_r$  suggest in water

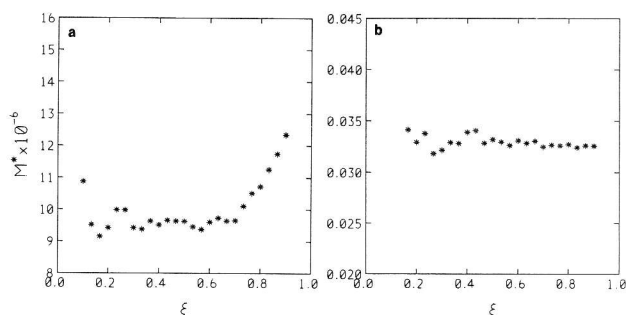


**Figure 3.** Plots of  $M^*$  as a function of  $\xi$ : (a) Copo 9 in water; (b) Copo 9 in chloroform. Other details as in Figure 1.

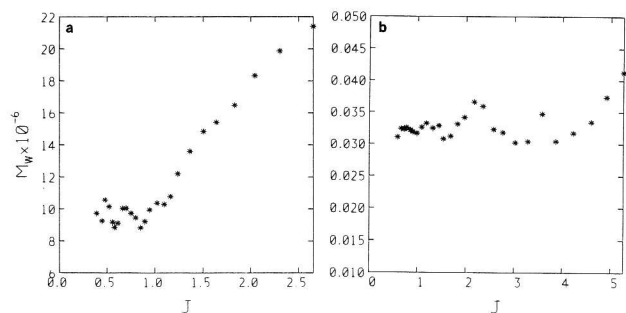


**Figure 4.** Plots of point average molecular weights  $M_w$  vs (fringe) concentration  $J$ : (a) Copo 9 in water; (b) Copo 9 in chloroform. Other details as in Figure 1.

an aggregation number of the unimer into "micelles" of approximately  $430 \pm 80$  residues per aggregate.

Plots of point weight-average molecular weights  $M_w$  vs  $J$  also reveal that Copo 9 is considerably less polydisperse as a unimer in  $\text{CHCl}_3$  (Figure 4b) compared to the case of micelles in water (Figure 4a).

## Discussion

These results illustrate how parallel experiments performed in different solvents can yield complementary information on a polymer system—even for cases of flotation. To extend the method to other optical systems<sup>9,19</sup> for the evaluation of number- and  $z$ -average molecular weights should be straightforward.

**Absorption Optical System.** This can only be applied to polymers that have an appropriate chromophore (e.g., lipoproteins, polyisoprenes). With this system a direct record of solute concentration vs radial displacement can be obtained without the problems of having to determine meniscii concentrations. The same treatment as described above for solute distributions recorded using Rayleigh optics can be applied.

**Schlieren Optical System.** The optical record is one of concentration gradient ( $dC/dr$ ) vs radial displacement  $r$  of the solute distribution at sedimentation equilibrium which is normally represented as a "Lamm plot", viz., a plot of  $\{1/r \ln(dC/dr)\}$  vs  $r^2$ . For the case of flotation the slope of this plot will be negative because of the negative buoyancy factor. The average slope gives the  $z$ -average (reduced) molecular weight over the whole solute distribution; local slopes give (reduced) point  $z$  averages, as with sedimentation equilibrium.  $z$ -Average molecular weights can be obtained from the (negative) reduced values via eq 2.

**Acknowledgment.** We are grateful to Mr. S. F. Ramzan for expert technical assistance and to Dr. A. J. Rowe for helpful comments. P.J.M. is grateful for a studentship from the SERC and financial support from Ciba-Geigy. This is Publication No. 77 from the ADDR Unit.

**Registry No.** (Ethylene oxide)(isoprene) (block copolymer), 122269-49-2.

(18) Crossley, J. M.; Spragg, S. P.; Creeth, J. M.; Noble, N.; Slack, J. *Biopolymers* **1980**, *21*, 233.

(19) Lloyd, P. H. *Optical Methods in Ultracentrifugation, Diffusion & Electrophoresis*; Oxford University Press: London, 1974.